Revisiting the Fibonacci spiral pattern for stiffening rib design

L. Meng and J. Zhang

**School of Mechanical Engineering,
Northwestern Polytechnical University, China**

Abstract

For a long period, phyllotaxis (the arrangement of leaves on a plant stem) has been observed as an interesting morphological property of various plants, and the phyllotactic spirals form a distinctive class of patterns in nature. These days, the unique patterns governed by the Fibonacci sequence, or the golden ratio in a deeper sense, have moved beyond the botanical system and came to be universal, occurring in architectural and structural design. In this work, we develop a design approach for curvilinear stiffening ribs which follow the Fibonacci spiral pattern. The parametric model of the designed ribs is built according to two parameters, one discrete and another continuous. Parametric studies on the two variables are performed to assess the potential mechanical advantages of the Fibonacci spiral pattern in stiffening structures. The deformation-, vibration- and buckling-resisting capacities are investigated for thin-walled stiffening plates with a central cut-out. Moreover, an attempt is devoted to clarifying the rationality of curvilinear employment in other designs. Lastly, we demonstrate that the developed protocol does not limit itself to planar structures with cut-outs, and it is easy to be extended to stiffening ribs on curved surfaces, where the gain in mechanical property is observed to be even more visible and pronounced.

Keywords: Fibonacci spiral, stiffening ribs, thin-walled structure, phyllotaxis, structure design, bucking

1 Introduction

In recent decades, rib-reinforced shell structures have found attractive applications in aerospace engineering, given their unique light-weight nature as well as the outstanding load-bearing capacity[1]. On the other side, stiffened structures were reported to feature satisfactory dynamic properties compared to their thin-walled counterparts[2].Hence, the layout and orientation design of stiffeners has long been a research interest in the realm of light-weight design of high-performance components, and fruitful results have been extensively reported[3].

We intend to develop in the present work a novel parametric design approach for the stiffened thin-walled structures with im-proved mechanical properties. To alleviate the tedious reconstruction after traditional topology optimization, the proposed parametric approach should enable the stiffener layout to be optimized with a limited number of variables and guarantee a ready-to-fabricate design. Specifically, the stiffeners are meticulously designed to follow the Fibonacci spiral pattern, reminiscent of the biological settings frequently encountered in nature. For example, seeds of sunflowers, branching in trees, and arrangement of leaves on a stem all take similar spiral patterns in clockwise and counter-clockwise directions, the spiral numbers of which are consecutive in the Fibonacci series, Fig.1a[4].

In fact, the Fibonacci spirals and the Fibonacci numbers have aroused scientific urges since antiquity. However, still today, it is non-trivial to answer the question "How is the Fibonacci spiral pattern formed?", and the fundamental rules seem to re-main unrevealed. Notwithstanding that, we deem that biochemistry, mechanics, and even physics shall all play a role in generating the unique patterns[5,6]. Among these, the mechanical aspects were convinced to play a significant role in pattern formation[7]. Continuous efforts have been devoted for decades[8,9].

On the basis of the reviewed development, it is remarked that the underlying mechanisms of the Fibonacci spiral pattern in nature still remain elusive, given the coupled effect of energy, nutrition transportation, and mechanics. Albeit that, we would like to formulate another issue of the problem:" Can the Fibonacci spiral pattern be employed in stiffening ribs design and to what extent will it improve the resulting mechanical properties of the designed structure?" With this in mind, we explore in this work the possibility of adopting the Fibonacci spiral pattern in stiffening structures, and to examine carefully potential improvements in load-bearing and other mechanical performances.

2 Methods

As widely recognized, the mathematical basis for the Fibonacci/phyllotactic spiral is directly related to the Fibonacci sequence and to the golden angle ϕ . Both mathematicians and biologists have proven that this angle is highly sensitive to the separation of individual primordial or to the packing density of florets, and it measures approximately $137.5°$, or, $(3-\sqrt{5})\pi$ radians more precisely. To generate the

Fibonacci spirals, a series of N key points are required. Using a mathematically idealized form of phyllotaxis, the coordinates of the key points lying on the Fibonacci spiral can be expressed in relatively simple circular functions as:

$$\begin{cases} x_i = r_i \cdot \cos((i-1) \cdot \phi) \\ y_i = r_i \cdot \sin((i-1) \cdot \phi) \end{cases}$$

(1)

where i is the key point index. r_i, the radius of the current point to the center of growth, is generally defined as $r_i = \sqrt{i}$ according to the formulation devised by Helmut Vogel (1979). Notice that, for the sake of a more flexible design, we suppose a linear expansion pattern of the key points/florets. A constant growth factor $\delta r = const$ is adopted in the current work, giving $r_i = r_{i-1} + \delta r$. Fig. 2 schematically illustrates the generation of 50 key points that lie on the Fibonacci spirals.
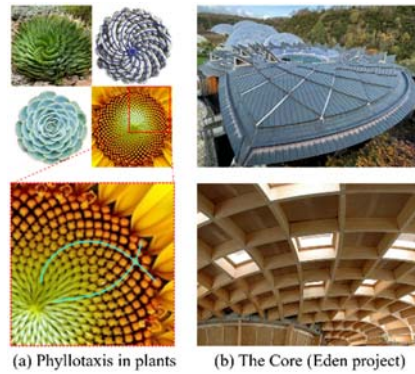
Figure 1: Fibonacci spiral patterns in nature and architectural design: (a) clockwise and anti-clockwise spirals in plants such like Aloe polyphylla and sunflower, (b) Fibonacci pattern seen in the Core's ceiling.
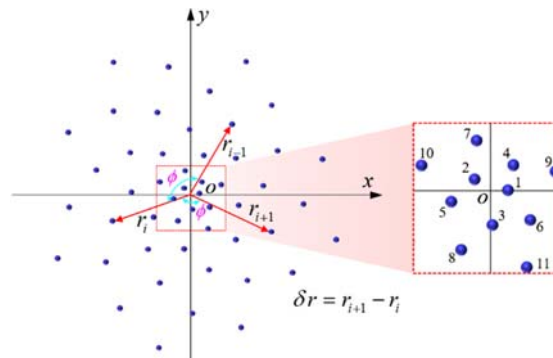
Figure 2: Schematics of the generation of 50 'florets' that lie on the Fibonacci spirals. The involved parameters are r1 = 5 and $\delta r = 2$.

Upon the generation of Fibonacci spirals, geometric models of stiffening ribs can then be readily achieved in commercial CAD software such as Siemens NX Unigraphics. The most popular way is to assign a rectangular cross-section to the frame lines. Either, other user-defined profiles can be realized via plug-in development. A series of Boolean operations or confine transformations can as well

3

be employed to generate more complex engineering parts. Fig. 3 illustrates the procedures to stiffen a perforated rectangular plate with ribs of Fibonacci spiral patterns.
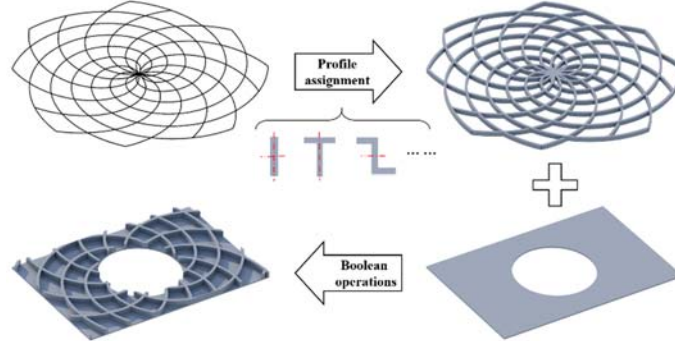
Figure 3: Generation of a thin-walled plate with a circular cut-out, stiffened by Fibonacci spiral pattern ribs.

By varying the number of spiral lines, four stiffening strategies are pro-posed and are demonstrated in Fig. 4a. As can be observed, the pair of parastichy is one of the governing parameters that may alter the topological layout of the stiffeners. Meanwhile, due to the integral nature of this pair, the topological evolution of stiffeners is discontinuous. Further to this comparison, the morphology evolution of the stiffening ribs according to the growth factor δr is also studied. Fig. 4b includes another four stiffening plates with varying δr. It is pointed out that, different from the pair of parastichy, δr is continuous and the ribs evolve in a smoother manner. As can be observed from the figure, δr is closely correlated with an amplification factor of the structure. To be specific, increasing the growth factor is almost equivalent to applying a "zoom-in" operation on the ribs. Furthermore, we emphasize that the growth factor can alter the topology of the stiffener as well, since the magnified Fibonacci spirals are ultimately trimmed by the bounded structural boundaries, and topological change is in fact allowed.
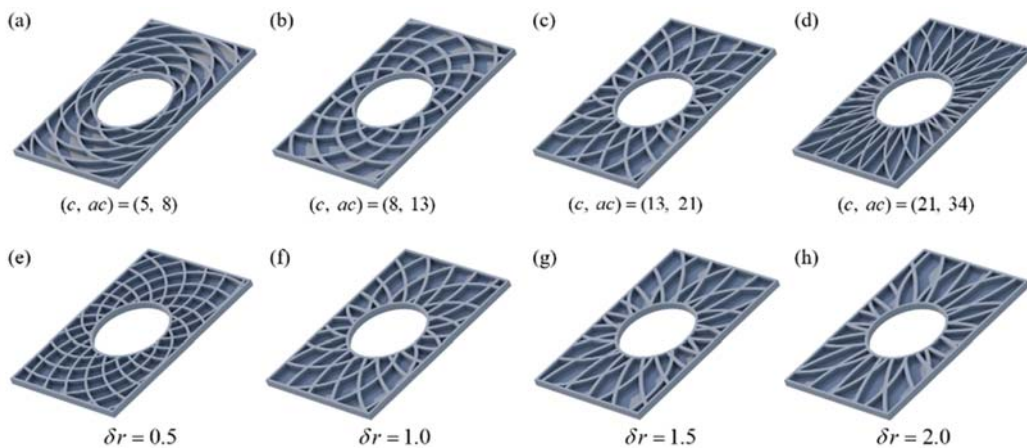
Figure 4: different reinforced plates with Fibonacci spiral ribs defined by: (a)-(d) diverse pairs of parastichy (with fixed growth factor δr = 1.0) and (e)-(h) diverse growth factorsδr (with fixed pair of parastichy (c, ac) = (13, 21))

3   Results

3.1   Deformation-resisting capacity analysis

The introduction of ribs encourages improved performances of thin-walled structures from diverse views, among which are the load-bearing, vibration-and buckling-resisting capacities. With the aim of revealing the potential tunability of Fibonacci spiral pattern ribs in mechanical performances, weexplore in this section the performance improvement of stiffened rectangularplates in various manners. For the generation of Fibonacci pattern ribs,four pairs of parasiticy are selected: (5,8), (8,13), (13,21), and (21,34). Thegrowth factor is varied from 0.3 to 2.1, with a step length of 0.2, providinga total of 40 stiffening strategies. For comparison reasons, we also includein the model set square- and X-grid counterparts, each with two different densities of stiffeners, as illustrated in Fig. 5.

(a)   (b)   (c)
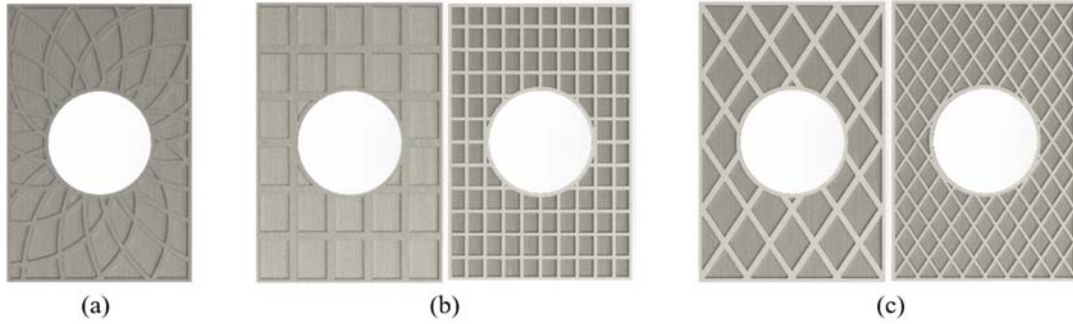
Figure 5: Stiffening patterns considered in the current work: (a) one of the 40

Fibonacci spiral patterns, with the governing parameters for the other models presented in Tab.1, (b) the two square-grid patterns, and (c) the two X-grid patterns.
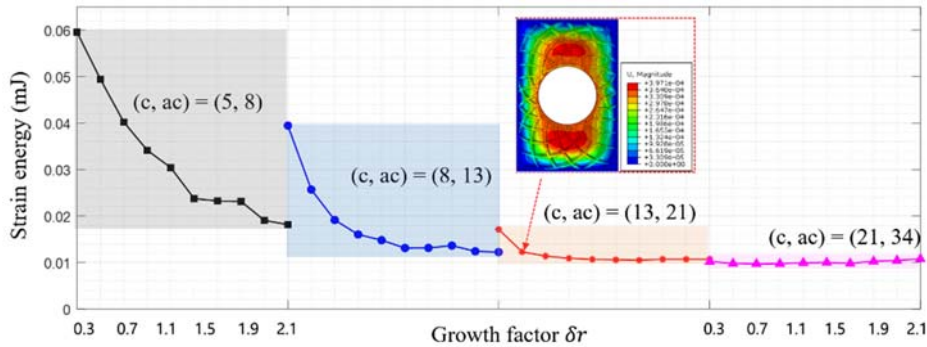
Figure 6: Comparison of the strain energy measured on plates stiffened according to the Fibonacci spiral patterns. The topology of the stiffening ribs is controlled by the pairs of parasiticy (c, ac) as well as the continuously evolving growth factor δr from 0.3 to2.1. The inset shows the displacement field of the design with a satisfactory stiffness, (c, ac) = (13, 21) and δr = 0.5.

We investigate in the first place the capability of different stiffening pat-terns in improving the overall stiffness of the plate. For such purpose, a dis-tributed load of 100N is applied along the normal direction of the stiffened panels, the outer boundary of which is fully clamped. Such load condition mimics that of a pressure vessel and is of practical sense. We have chosen structural compliance (i.e., the strain energy) as a characteristic measure of the stiffness of stiffened parts. Unlike the maximum displacement which be-longs to a localized description, the strain energy better indicates the overall deformation-resisting performance of parts under loading. Fig. 6 plots the strain energy stored on the plate as a function of the growth factor of the Fibonacci spiral pattern.

	Fibonacci-pattern	Square grid pattern		X-grid pattern	
		Dense	Coarse	Dense	Coarse
Compression	0.0123	0.0295	0.0292	0.0233	0.0218
Shear	0.0343	0.0349	0.0339	0.0373	0.0363
Torsion	0.0027	0.0033	0.0032	0.0027	0.0031

Table 1: Compliance of stiffened panels under three loading conditions. The values listed for the Fibonacci pattern stiffened plates correspond to the pattern in the inset of Fig.8.Values in the table are in [mJ].

To better evaluate the stiffening effect brought about by the Fibonacci spiral pattern ribs, we further calculate the stain energy of reinforced plates by square- and X-grid ribs. For the sake of completeness, the capabilities in resisting shear and torsion load have also been investigated for the three stiffening patterns. A torque of $10kN \cdot m$ has been applied to the central cut-out with the four edges fully clamped. As to the shear load, the bottom edge is fixed while a shear force of 1kN is applied to the upper edge. Notice that, structural compliance has been adopted as the mechanical figure of merit for a uniform characterization of stiffness, and that corresponds to the compression loading has been included as well in Tab.1. Particularly, for the Fibonacci spiral pattern, the strain energy values included for comparison correspond to that of the pattern as shown in the inset of Fig.6.

As can be concluded, the Fibonacci spiral pattern ribs render the highest stiffness to the panel under a distributed compression, with the strain energy being half of its grid-stiffened counterparts. Also, a slightly better shear-resisting performance is credited to the Fibonacci-pattern panels, given the limited discrepancy in the values. Furthermore, the Fibonacci pattern stiffened panel is observed to store the least strain energy when the same torque is applied to the central cut-out, implying simultaneously the best torsion-resisting performance. In all, the Fibonacci spiral stiffening pattern is noticed to lead to an excellent deformation-resisting performance under the three loading cases, allowing it to be served as a feasible alternative in the reinforcement of thin-walled engineering parts. We should emphasize that the above conclusion may be slightly altered by the boundary conditions as well as the dimensions of the structure.

3.2 Buckling-resisting capacity analysis

We then investigate the buckling-resisting capacities of all the 40 Fibonacci patterns and 4 grid pattern stiffened plates. The 4 geometric models of grid-stiffened panels have been previously demonstrated in Fig.7, while that of the Fibonacci pattern stiffened panels have been omitted for clarity's sake. We should emphasize again that the same structural weight is maintained for all the cases with the aim of a fair comparison, and this is realized by controlling the width of the ribs in respective cases.

Three load conditions are considered: distributed vertical load, concentrated load locally applied to the central cut-out, and torsion load acting on the central cut-out. For clarity's sake, these three load conditions are denoted by "Load A", "Load B", and "Load C", respectively. Readers are invited to note that, the three loading conditions have been schematically demonstrated in Fig.7 accompanied by three different patterning strategies. We emphasize in the meantime that, for each individual structure, the buckling resisting capacity has been analyzed with all the above three loading cases.
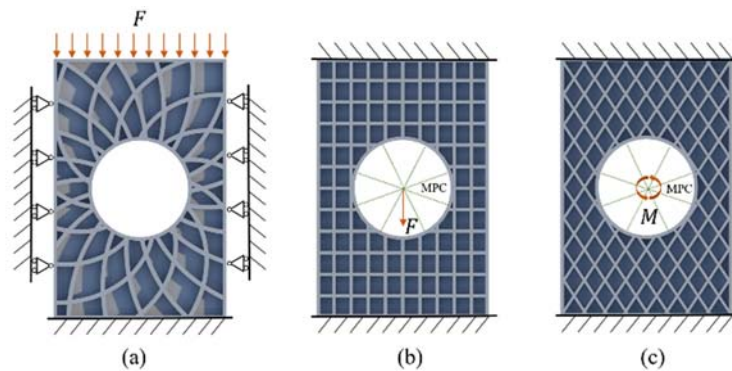
Figure 7: Loading conditions for comparison of buckling-resisting capacities of various stiffened plates: (a) vertical distributed load, (b) concentrated load, and (c) torsion load at the central cut-out.

In this subsection, linear buckling analysis is conducted. For simplicity, the unit load is generally applied on the part such that the buckling-load factors (BLF) provide a direct estimation of the buckling-load magnitude. Notice that Load A and B are in N while Load C is in $N \cdot m$. Tab. 2 summarizes the critical buckling loads of various panels under different load conditions. It is pointed out that the values listed for the Fibonacci pattern stiffened plates are the biggest ones chosen among the 40 models, implying the best buckling-resisting performance within the searched design domain.

As can be concluded from the results, the Fibonacci pattern outperforms the other two types of stiffening ribs when a unit concentrated force is applied at the central cut-out (by adopting the multi-point constraint, MPC), with an improvement of buckling-resisting capacity by 8% and 14%, respectively. If a vertically distributed load is applied at the two far ends of the plate, the Fibonacci pattern ribs demonstrate as well a satisfactory performance with the critical buckling load being 509KN. However, in such circumstances, the X-grid ribs provide the least support to resist

buckling deformation. This is attributed to the fact that more material is desired to be placed along the load-carrying path in buckling-resisting design. As for Load C, an outperformance is marked for the Fibonacci spiral pattern ribs than the square-grid ribs, improving the critical buckling load from 351 to 391 KN, and the X-grid pattern shows the best buckling-resisting performance. This is reasonable since the cross-cutting is favorable for torsion load and it transfers load more directly to the fixed boundary.

	Fibonacci-pattern	Square grid pattern		X-grid pattern	
		Dense	Coarse	Dense	Coarse
Load A	509347	542225	481765	439672	423538
Load B	1020600	989354	637413	919124	891582
Load C	39143500	35735700	34668400	41400300	41319300

Table 2: Critical buckling loads of various plates stiffened by different strategies. Load A refers to the vertically distributed load, Load B, a central concentrated load, and Load C, a torsion moment (units in N and N · m).

We notice as well that the critical buckling loads are sensitive to patterns of stiffening ribs. Overall, the X-grid ribs are more suitable for torsion loads, while the square-grid pattern is preferable in the other two loading cases. Notice as well that the density of X-grid ribs seems to less affect the buckling resisting capacity, since the critical loads differ only within 5% for sparsely and densely distributed ribs. However, adjusting the density of square-grid ribs can change significantly the buckling-resisting capacity.

It is observed that, for all three load conditions, the best topology of the stiffening ribs is generated on top of 21 clockwise and 34 anti-clockwise Fibonacci spirals, Fig. 8. However, the growth factors are slightly different, being 0.3, 1.1, and 0.5 respectively for the three structures. Furthermore, we notice that the first eigenmodes are not necessarily symmetry. This is due to the asymmetry nature of the Fibonacci spiral pattern.
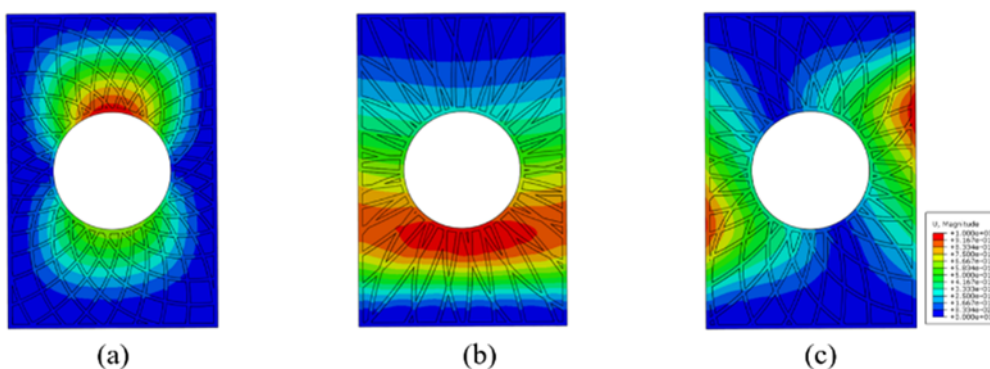
Figure 8: First eigenmodes of Fibonacci-pattern stiffened plates demonstrating the best buckling resisting performance under various loading conditions: (a) $\delta r = 0.3$ for Load A, (b) $\delta r = 1.1$ for Load B, and (c) $\delta r = 0.5$ for Load C.

4   Conclusions and Contributions

In this work, we have revisited the Fibonacci spiral patterns that are frequently observed in nature and explored thoroughly their possible integration into the design of stiffening ribs on thin-walled structures. The concise modelling of Fibonacci pattern ribs using only two intrinsic parameters has been demonstrated. A series of finite element simulations, covering quasi-static, modal, linear and nonlinear buckling analysis, has revealed the wide tunability of the mechanical performances of the design. The advantage of the Fibonacci spiral pattern reinforced 3D reflector structure has been demonstrated both numerically and experimentally. As part of broader outreach efforts, we also demonstrated that the curvilinear ribs may not necessarily be advantageous. Rather, straight ribs can be more helpful where the stress status is simple and a more direct load-carrying path is desired. In other cases, curvilinear ribs may render better mechanical performances by aligning themselves with the load-carry path under a complex load condition. Anyhow, the proposed Fibonacci spiral pattern is promising in finding its engineering applications given its diversity in generating both curvilinear and quasi-straight ribs.

References

[1]   L. Meng, W. Zhang, D. Quan, G. Shi, L. Tang, Y. Hou, P. Breitkopf, J. Zhu, T. Gao, From topology optimization design to additive manufacturing: Today's success and tomorrow's roadmap, Archives of Computational Methods in Engineering 27 (2020) 805–830.

[2]   H. Wu, A. Liew, T. Van Mele, P. Block, Analysis and optimisation of a rib-stiffened vaulted floor for dynamic performance, Engineering Structures 213 (2020) 110577.

[3]   W. Zhang, L. Jiu, L. Meng, Buckling-constrained topology optimization using feature-driven optimization method, Structural and Multidisciplinary Optimization 65 (2022) 1–20.

[4]   Z. Sun, T. Cui, Y. Zhu, W. Zhang, S. Shi, S. Tang, Z. Du, C. Liu,R. Cui, H. Chen, et al., The mechanical principles behind the golden ratio distribution of veins in plant leaves, Scientific Reports 8 (2018)1–8.

[5]   S. Strauss, J. Lempe, P. Prusinkiewicz, M. Tsiantis, R. S. Smith, Phyllotaxis: is the golden angle optimal for light capture, New Phytologist 225 (2020) 499–510.

[6]   P. Prusinkiewicz, T. Zhang, A. Owens, M. Cieslak, P. Elomaa, Phyllotaxis without symmetry: what can we learn from flower heads, 2022.

[7]   C. R. Steele, Shell stability related to pattern formation in plants, J. Appl. Mech. 67 (2000) 237–247.

[8]   G. J. Mitchison, Phyllotaxis and the fibonacci series: An explanation is offered for the characteristic spiral leaf arrangement found in many plants., Science 196 (1977) 270–275.

[9]   P. D. Shipman, A. C. Newell, Phyllotactic patterns on plants, Physical review letters 92 (2004) 168102.